Cerebral Cortex April 2010;20:953-965
doi:10.1093/cercor/bhp157
Advance Access publication August 14, 2009

Distinct and Overlapping Functional Zones in the Cerebellum Defined by Resting State Functional Connectivity

Jill X. O'Reilly[1], Christian F. Beckmann[1,2], Valentina Tomassini[1,3], Narender Ramnani[4] and Heidi Johansen-Berg[1]

[1]FMRIB Centre, Department of Clinical Neurology, University of Oxford, OX1 9DU Oxford, UK, [2]Division of Neuroscience and Mental Health, Imperial College, SW7 2AZ London, UK, [3]Department of Neurological Sciences, "La Sapienza" University, 00185 Rome, Italy and [4]Department of Psychology, Royal Holloway, University of London, TW20 0EX London, UK

Jill X. O'Reilly and Christian F. Beckmann contributed equally to the work.

The cerebellum processes information from functionally diverse regions of the cerebral cortex. Cerebellar input and output nuclei have connections with prefrontal, parietal, and sensory cortex as well as motor and premotor cortex. However, the topography of the connections between the cerebellar and cerebral cortices remains largely unmapped, as it is relatively unamenable to anatomical methods. We used resting-state functional magnetic resonance imaging to define subregions within the cerebellar cortex based on their functional connectivity with the cerebral cortex. We mapped resting-state functional connectivity voxel-wise across the cerebellar cortex, for cerebral–cortical masks covering prefrontal, motor, somatosensory, posterior parietal, visual, and auditory cortices. We found that the cerebellum can be divided into at least 2 zones: 1) a *primary sensorimotor zone* (Lobules V, VI, and VIII), which contains overlapping functional connectivity maps for domain-specific motor, somatosensory, visual, and auditory cortices; and 2) a *supramodal zone* (Lobules VIIa, Crus I, and II), which contains overlapping functional connectivity maps for prefrontal and posterior-parietal cortex. The cortical connectivity of the supramodal zone was driven by regions of frontal and parietal cortex which are not directly involved in sensory or motor processing, including dorsolateral prefrontal cortex and the frontal pole, and the inferior parietal lobule.

Keywords: cerebellum, fMRI, functional connectivity, networks, resting-state

Introduction

The cerebellum, traditionally considered a motor structure, is increasingly understood to play a broader role by virtue of its interactions with association cortex such as the parietal and prefrontal lobes. This shift has been driven by functional imaging and patient work in humans, and by anatomical studies in monkeys. Since the earliest days of functional imaging, cerebellar activations have been observed, often unexpectedly, in experiments with minimal motor demands including sensory (Gao et al. 1996; Blakemore et al. 1999) and linguistic tasks (Roskies et al. 2001; Noppeney and Price 2002; Xiang et al. 2003; Ravizza et al. 2006) and in executive function (e.g., Desmond et al. 1997, 1998; for review see Stoodley and Schmahmann 2009). In parallel, patient studies indicate wide-ranging cognitive deficits following cerebellar damage, including altered social and emotional behavior and a slowing of mental performance (e.g., Schmahmann and Sherman 1998; Schmahmann and Caplan 2006).

The functional heterogeneity of the cerebellum is reflected in its connectional heterogeneity: The cerebellum has both afferent and efferent connections with diverse regions of cerebral cortex including the somatosensory (Glickstein et al. 1985; Schmahmann and Pandya 1992), visual (Schmahmann and Pandya 1992, 1993; Glickstein et al. 1994), auditory (Schmahmann and Pandya 1991, 1992), parietal (Schmahmann and Pandya 1993; Clower et al. 2005), and prefrontal areas (Schmahmann and Pandya 1997; Middleton and Strick 2001; Kelly and Strick 2003) as well as primary motor and premotor cortex.

Anatomical studies in monkeys suggest that different cerebral–cortical projections form discrete "channels" and should therefore map onto different regions of the cerebellar cortex. Afferent fibers destined for the pontine nuclei (the cerebellar input nuclei) are segregated within their white-matter bundles by cortical region of origin (Schmahmann and Pandya 1992), and retain this segregation in the pontine nuclei (Brodal 1978). Similarly, cerebellar efferents arising in the dentate nucleus are organized according to the functional topography of the cerebral cortex (Dum and Strick 2003). In one particularly important study in monkeys, Kelly and Strick (2003) identified the polysynaptic connections between 2 cerebral–cortical areas, the primary motor cortex and area 46 of the prefrontal cortex, and specific territories in the cerebellar cortex. Cerebellar lobules HIV, HV, HVI, and HVIII were found to be interconnected with the primary motor cortex (a later study by Lu et al. (2007) indicated that M1 also receives projections from Crus I). (We have followed the nomenclature of Schmahmann et al. (2000), "MRI Atlas of the Human Cerebellum" in which the cerebellar lobules are labeled I-X from the anterior/superior border of the cerebellum, through posterior, to the anterior/inferior border. Schmahmann's nomenclature was partly based on that of Larsell [e.g., Larsell and Jansen 1972], in which the cerebellar hemispheres were distinguished from the vermis with the prefix H. We have included the H prefix where we are referring specifically to activity in the hemispheres, and the prefix "vermal" where we are referring specifically to vermal activity. Where we are referring to the whole lobule, we use no prefix.) In contrast, parts of Lobule VIIa, especially Crus II, were interconnected with prefrontal area 46. Importantly, the cerebellar-cortical regions which received input from each cortical area were found to send output back to the same cerebral area, forming parallel connectivity loops. In view of these results, Strick and colleagues have proposed that cerebro-cerebellar connectivity is characterized by discrete "parallel circuits," reciprocally linking different parts of the cerebellum with their corresponding cerebral–cortical functional areas (e.g., Dum et al. 2002).

However, despite extensive work mapping cortical connections with the pontine nuclei and dentate, the connectional

topography of the cerebellar cortex itself (in relation to the cerebral cortex) remains largely unmapped. Anatomical tracer studies of cerebro-cerebellar connectivity have almost exclusively focused on the input and output nuclei of the cerebellum, because of the difficulty in tracing the multisynaptic circuits which link cerebellar and cerebral cortices (Kelly and Strick 2000). Projections from the cerebral cortex synapse in the pontine nuclei, then the cerebellar cortex; reciprocal connections synapse first in the cerebellar dentate, then the thalamus, before reaching the cerebral cortex. Very few studies have successfully traced connections trans-synaptically from cerebral to cerebellar cortex (Kelly and Strick 2003; Lu et al. 2007). Furthermore, diffusion tractography, an imaging method that can provide information on anatomical connectivity in the human brain, is at present problematic between the cerebellum and the cerebral cortex for 3 reasons. First, cerebellar afferents and efferents decussate in regions of dense crossing fibers in the brainstem. Second, cerebellar efferents pass through a "bottleneck" in the superior cerebellar peduncle which is so narrow that its subregions cannot clearly be distinguished with the spatial resolution of diffusion imaging. Third, cerebellar-efferents synapse in areas of gray matter (notably the thalamus) before reaching the cerebral cortex. Finally, all anatomical studies face the difficulty that each region of cerebellar cortex receives inputs via at least 2 routes, relayed by either the pontine nuclei or the inferior olive.

Given the difficulty of tracing cortico-cerebellar anatomical connections "cortex to cortex," it is at present difficult to relate our knowledge of the connectivity of the cerebellar input and output nuclei to a *functional* topography of the cerebellar cortex. In accordance with the anatomical data of Kelly and Strick (2003), sensorimotor representations of the body have been found in the superior/anterior-most part of the cerebellum (lobules III–V or VI) and in lobule HVIII (MacKay and Murphy 1973; Ojakangas and Ebner 1994; Gao et al. 1996; Jueptner et al. 1997; Thickbroom et al. 2003). However, using functional methods it is much more difficult to be specific about which areas of association cortex (prefrontal and posterior-parietal cortex) are linked with a cerebellar subregion because the functional roles of the cerebral–cortical areas in question are less clearly defined—there is probably no single task we could give to a monkey which, if associated with activity in a cerebellar neuron, would allow us to conclude that we had found a "cerebellar prefrontal" or "posterior-parietal" cell. Indeed, functional imaging studies indicate that the prefrontal cortex is generally active as part of a broad network of association cortex. Based on patient work, Schmahmann and colleagues (Schmahmann 1996, 2004; Schmahmann and Sherman 1998) have described a schema in which the posterior lobe of the cerebellum is involved with cognitive or executive functions: "in patients with lesions involving the posterior lobe of the cerebellum…[they observed] impairment of executive functions such as planning, set-shifting, verbal fluency, abstract reasoning and working memory; difficulties with spatial cognition including visual–spatial organization and memory…" (Schmahmann and Sherman 1998)—but again, the executive functions described are not exclusively associated with one region of the cerebral cortex.

Despite these difficulties, an understanding of connectivity with the cerebral cortex is particularly important in the case of the cerebellum because the function of its subregions may be defined by their connectivity. The combination of the connectional diversity of the cerebellum with the extreme uniformity of cerebellar microcircuits fits a model in which the cerebellum applies a particular *computational* function to information from a range of cortical areas, rather than having a functional specialization itself—motor, cognitive, or otherwise (Eccles et al. 1967; Bloedel 1992; Schmahmann and Sherman 1998; Ramnani 2006; Ito 2008).

In the present study, we used resting-state functional magnetic resonance imaging (fMRI) to probe the topography of cerebral–cortical connectivity in the cerebellar cortex. This functional connectivity approach uses fMRI data acquired while the subject is at rest. The concept behind resting-state fMRI is that when the brain is "free-wheeling" (not involved in an externally cued task), correlations in slowly fluctuating spontaneous brain activity tend to reflect the intrinsic functional networks of the brain (Biswal et al 1995; see Fox and Raichle 2007 for review). For example, cortical areas typically associated with motor function show a significant degree of covariation and are therefore thought to form a particular "resting state network" (RSN) while cortical areas associated with visual processing form a separate RSN (Beckmann et al. 2005). Independent components analysis indicates that a large percentage of the fMRI signal in the resting human brain can be explained in terms of just a few (8–10) RSNs (Damoiseaux et al. 2006). These primary RSNs are highly consistent across time and space and between individuals, suggesting they represent something fundamental about the functional organization of the brain. Further discussion of the resting-state approach and its advantages and caveats is given in the Discussion.

We mapped resting-state functional connectivity voxel-wise across the cerebellar cortex for a set of cortical regions or masks. The result of this analysis was a set of correlation maps across the cerebellar cortex, representing resting functional connectivity with each of a number of cortical regions. The approach used in this study is particularly useful for investigating whether subdivisions exist within a structure, because mapping within the structure of interest is voxel-wise. We defined a set of cerebral–cortical masks representing known functional systems, and tested the correlation of each cerebellar voxel with these cortical masks. In contrast, a typical resting-state approach would be to divide the cerebellum into regions a priori, and then use the cortical RSNs associated with each cerebellar region to infer its function or connectivity. The present approach is similar to that introduced by Zhang et al. (2008) to map thalamo-cortical connectivity. We used the method to address a series of specific hypotheses about cerebro-cerebellar connectivity.

First, we asked whether separate motor and prefrontal zones could be defined in the cerebellar cortex, based on resting functional connectivity. The motivation for this analysis was to replicate the findings of Kelly and Strick (2003, described above) with the resting state method; the division between motor and prefrontal also reflects the broad distinction between motor and executive zones proposed by Schmahmann (Schmahmann and Sherman 1998).

Second, we further probed the validity of the resting-state approach through the lateralization of correlations. The white matter connections between the cerebellum and the cerebral cortex are crossed, so if resting-state correlations reflect neural connectivity, the correlation maps should show a contralateral organization, with voxels in the left cerebellum correlating

more strongly with right cortical regions and vice versa. Such contralateral relationships are much more likely to be neural than vascular in origin. We might a priori expect artifactual (non-neurally generated) correlations to be stronger in the nearer, ipsilateral hemisphere. We therefore compared the correlation maps for left- and right-hemisphere cortical masks (using motor and prefrontal cortical masks as above).

Third, we asked how the broad distinction between motor and prefrontal zones related to other cortical areas. We extended the set of cortical masks to 6 large zones, representing different functional systems (prefrontal cortex, motor and premotor cortex, somatosensory cortex, posterior-parietal cortex, superior temporal cortex, and visual area middle temporal [MT]). Between them, the masks covered the regions of cortex reported to have significant cerebellar-afferent connections with neurons in the pontine nuclei or cerebellar-efferent connections with the dentate in nonhuman primates (see above).

Finally, we focused on the connectivity of the cerebellum with supramodal association cortex (prefrontal and posterior-parietal cortex), and asked which subregions *within* the prefrontal and posterior-parietal masks contributed to the correlation patterns we observed in the cerebellum. The motivation for this analysis was that some researchers (Glickstein 2007) have suggested that only the subregions of prefrontal and parietal cortex which are involved in motor control are linked to the cerebellum. If this were the case, we would expect to see the strong correlation with the cerebellar supramodal zone in the frontal eye fields and/or area 8 in the case of the prefrontal cortex mask, and for the parietal cortex, the anterior intraparietal cortex (aIP), which is involved in grasping, and superior parietal lobule which contains many regions involved in the planning of action, thought to be the homologs of monkey intraparietal sulcus (IPS) regions (see Culham and Valyear 2006 for review) including lateral intraparietal area (LIP; eye movements), medial intraparietal area (MIP; reaching), and ventral intraprietal area (VIP; movements in head centered space).

In the Supplementary Information, we present additional analyses mapping correlation with the Eigen time series of each mask across the cerebral cortex. These additional analyses give a picture of which regions within each mask contribute most strongly to the correlations described below, and indicate the strength of correlation between the cortical masks.

Materials and Methods

We performed a series of analyses investigating the contrasts between different sets of masks. These are presented as Analyses 1–4 below. The procedures which were common to all analyses are presented only in Analysis 1.

Analysis 1. Motor and Prefrontal Zones in Cerebellar Cortex

Data Acquisition

We collected resting-state fMRI data and anatomical scans for 12 healthy volunteers (9 females, age range [mean ± SD] 43.08 ± 9.17, range 31–61) who participated in the experiment in accordance with ethical approval from the UK Central Office for Research Ethics Committees.

During the 11-min scan, participants lay supine in a 1.5 T Siemens Sonata MR scanner. They were instructed to close their eyes and lie still. Cushions were used to reduce head motion. Whole-brain blood oxygen level–dependent (BOLD) fMRI data sets were collected, using the following parameters: 45 axial slices, in-plane resolution 3 × 3 mm, slice thickness 3 mm, no gap, repetition time = 3400 ms, echo time = 41 ms, 200 volumes.

A structural scan was acquired for each participant, in the same session, using a T_1-weighted 3D FLASH sequence (repetition time = 12 ms, echo time = 5.65 ms, and flip angle = 19°, with elliptical sampling of *k* space, giving a voxel size of 1 × 1 × 1 mm in 5 min and 5 s).

Data Preprocessing

Data processing was carried out using tools from FMRIB Software Library, FSL (Smith et al. 2004). The first 6 volumes were discarded, then the following prestatistics processing was applied: motion correction using MCFLIRT (Jenkinson and Smith 2001); spatial smoothing using a Gaussian kernel of FWHM 6 mm; grand-mean intensity normalization of the entire 4D data set by a single multiplicative factor; high-pass temporal filtering (Gaussian-weighted least-squares straight line fitting, with sigma = 50.0 s, that is, at least half-power was retained for frequencies down to 0.01 Hz).

Masks

Cerebral–cortical and cerebellar masks were created in Montreal Neurological Institute (MNI) space by combining anatomical masks from the Harvard–Oxford Structural Atlas or Jülich Probabilistic Histological Atlas. The Harvard–Oxford atlas is a probabilistic atlas covering 48 cortical and 21 subcortical structural areas, available as a toolbox in FSLview. To create the atlas, T_1-weighted images of 21 healthy male and 16 healthy female subjects (ages 18–50) were individually segmented by researchers at the Harvard Centre for Morphometric Analysis using semiautomated tools developed in-house. The T_1-weighted images were affine-registered to MNI152 space using FLIRT (Jenkinson and Smith 2001), and the transforms then applied to the individual labels. These were combined across subjects to form population probability maps for each label. The Jülich Atlas is a probabilistic atlas created by averaging multisubject post-mortem cyto- and myelo-architectonic segmentations (Eickhoff et al. 2005). The atlas is based on the microscopic and quantitative histological examination of 10 human post-mortem brains. The histological volumes of these brains were 3D reconstructed and spatially normalized into MNI space. The Jülich atlas is also available as a toolbox in FSLview.

Cortical masks were transformed into the space of individual anatomical scans using nonlinear registration implemented with FNIRT (Andersson et al. 2007), and then into individual functional space using affine registration implemented with FLIRT (Jenkinson and Smith 2001).

In Analysis 1, masks were created for the prefrontal and motor/premotor cortex. The prefrontal mask included the entire lateral frontal convexity anterior to the precentral sulcus, including superior, middle, and inferior frontal gyri and the frontal pole. It included the medial aspect of the superior frontal gyrus and the medial aspect of the frontal pole. It excluded orbitofrontal cortex, the anterior cingulate and paracingulate gyrus, and the insula. The motor mask included the entire lateral cortex posterior to the precentral sulcus and anterior to the fundus of the central sulcus, and extended onto the medial surface as far as the paracingulate sulcus. The masks are shown in the top panel of Figure 1.

Voxel-wise Correlation Mapping

We used a voxel-wise approach to map resting-state functional connectivity across the cerebellar cortex, between each voxel in the cerebellar mask and characteristic time series associated with the cortical regions. First, we calculated the major Eigen time series representing activity in each of the cortical masks. The major Eigen time series is the single time series which best reflects coherent activity across the mask in that it represents the largest amount of variance across the set of voxels within the mask. We also calculated the major Eigen time series in masks representing the white-matter and cerebrospinal fluid (CSF; across the whole brain volume), which were derived using FSL tissue segmentation tool FAST (Zhang et al. 2001). Time series representing head motion were extracted using MCFLIRT (Jenkinson and Smith 2001). These 8 confound time series (white matter and CSF Eigen time series, plus 6 time series representing head motion) were regressed out prior to each analysis. The reason for regressing out white matter and CSF time series was to minimize the potential confounding effect of including non–gray-matter voxels in

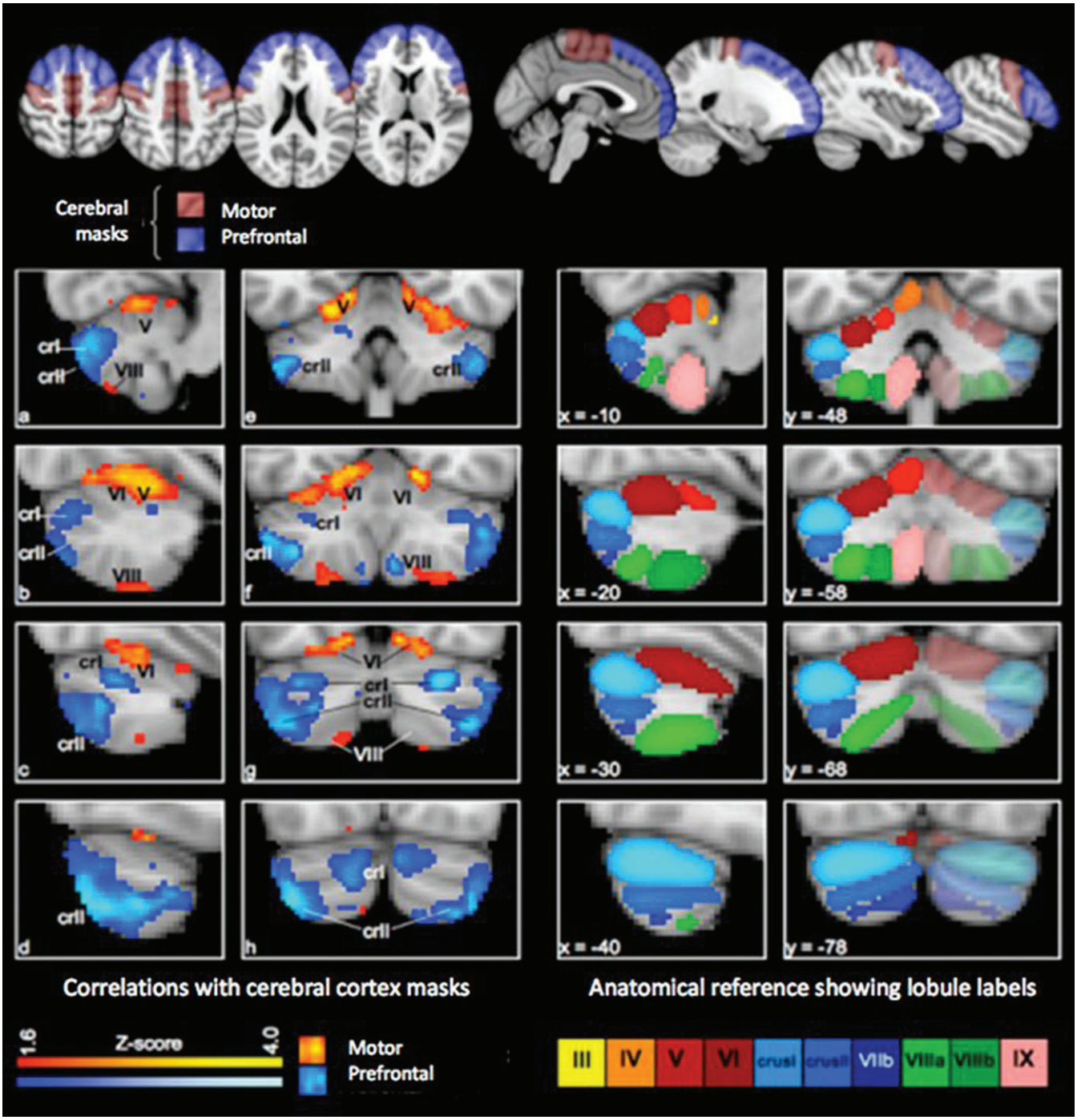

Figure 1. Correlation maps for motor and prefrontal cortex. Top panel: the cortical masks in standard (MNI) space. (Left 2 columns *a–h*) Correlation maps for the bilateral cortical masks in standard space, showing the voxel-wise significance (Z-score) of the correlation with prefrontal and motor regions in the cerebral cortex. Maps are thresholded at $Z > 1.6$ (equivalent of $P < 0.05$ uncorrected) and presented with the left cerebellar hemisphere to the left of the image. Note the clear division of the cerebellar cortex into prefrontal and motor zones. Right 2 columns show the lobular structure of the cerebellum, after Schmahmann (2000), for the slices shown to the left. Note the correspondence between Lobules IV–VI and VIII (red and green) with the motor zone, and Lobule VII (blue) with the prefrontal cortex. Abbreviations: crI, Lobule VIIa Crus I; crII, Lobule VIIa crus II; V, VI, VIII, Lobules V, VI, and VIII.

cerebellar and cortical masks, and to remove any non-tissue-specific confound effects such as global signal change.

Taking the preprocessed functional data, for each voxel in the cerebellar mask we calculated the partial correlation scores between its BOLD time series and the major Eigen time series for each cortical region, in each case regressing out the time series of all other cortical regions, so that the resulting correlation maps represented only correlations specific to the cortical mask in question. The output of the analysis took the form of correlation maps (across the cerebellum) in individual functional space, pertaining to each cortical mask.

The approach was similar to that used by Zhang et al. (2008) to map thalamocortical connectivity, with the exception that we used the first Eigenvariate to represent the time series of each cortical mask, whereas Zhang and colleagues used the mean time series of the mask. The Eigen time series approach has the advantage in terms of robustness, in that it represents the dominant time series (i.e., a time series which best

characterizes the majority of observed signal variation within the mask)—see Friston et al. (1996). As a Gedankenspiel, imagine 2 perfectly anticorrelated voxels of identical variance: in this case the mean would be constant and therefore fail to characterize the observed variations, whereas the Eigen time series fully describes the signal dynamics. Furthermore, it minimizes the danger that imprecise mask boundaries could allow tissue from adjacent regions with distinct functional profiles to contribute to the mask time course. In order to calculate this quantity, all voxels' time series within a given masks are assembled within a time × voxels matrix which, after removing the mean value per voxel, is then subjected to a Singular Values Decomposition in order to obtain the Eigen vectors of this matrix.

Group Analysis

Individual correlation maps were converted back into MNI space, first using an affine transformation from the space of individual functional to anatomical scans, then into MNI space using nonlinear registration implemented using FNIRT (as above). The standard-space correlation maps were entered into a group General Linear Model analysis using a fixed-effects approach. The resulting images (see Fig. 1) show *Z*-scores for the group correlation. *Z*-scores of peak voxels (see Tables 1–3) ranged from $Z = 1.96$ ($P < 0.025$) to $Z = 4.85$ ($P < 10^{-7}$). In order to estimate the full extent of overlap and segregation between the correlation maps for different cortical masks, a low threshold of $Z > 1.6$ was used (the equivalent of $P < 0.05$ uncorrected) for the images in Figures 1–3.

Analysis 2: Lateralization of Cerebro-cerebellar Connectivity

We divided the motor and prefrontal masks from Analysis 1 into left- and right-hemisphere masks. The 4 resulting masks were entered into a voxelwise correlation mapping as in Experiment 1. The data set was the same one used in Analysis 1. Preprocessing and analysis techniques were as in Analysis 1.

In addition to the voxelwise correlation mapping, we quantitatively probed the lateralization of connectivity in the following way. First we defined 4 anatomical regions of interest (ROIs) in the cerebellum—left- and right superior cerebellum (Lobules IV–VI) and left- and right Crus I/II. These regions were selected on the basis of the results of Analysis 1. We then calculated the mean correlation between voxels in the left- and right-superior cerebellum and the left- and right motor cortex, and between voxels in the left- and right Crus I/II and left and right prefrontal cortex. Correlations were calculated for each subject, excluding voxels with negative or zero correlation.

To test for significant lateralization of correlations, we compared the correlation of each cerebellar hemisphere with its 2 corresponding cortical masks (e.g., left Crus I/II with left prefrontal cortex vs. left Crus I/II with right prefrontal cortex). We then ascertained the statistical significance of the lateralization effect by a permutation test in which the data for the 2 cortical masks were randomly permuted 10 000 times (with each permutation representing an exchange of data for the left- and right-cortical masks in a random subset of subjects).

Analysis 3: Six Cortical Masks

We created 6 cortical masks, covering the regions of cerebral cortex in which connectivity with the cerebellum has been reported in anatomical tracer studies. The masks, which were bilateral, represented

Table 1

Peak correlation coordinates: motor and prefrontal target masks

Cerebellar lobule		*x*	*y*	*z*	*Z*-score
Prefrontal cortex					
Crus I	L	−36	−74	−46	4.46
	R	42	−72	−48	4.17
Crus II	L	−34	−66	−32	3.45
	R	28	−68	−30	4.25
Paravermal lobule VIIa	L	−6	−86	−32	3.42
	R	6	−82	−28	3.36
Lobule HIX (tonsil)	L	−8	−58	−56	2.29
	R	6	−58	−54	3.35
Motor/premotor cortex					
Lobule V	L	−14	−48	−14	3.68
	R	14	−46	−14	3.31
Lobule VI	L	−20	−60	−16	3.65
	R	18	−58	−14	4.00
Lobule VIII	L	−24	−54	−60	2.48
	R	28	−56	−58	2.54

Note: This table gives MNI coordinates for the voxel with the peak *Z*-score in each cluster for the correlation maps corresponding to motor and prefrontal cortex, that is, the results of Analysis 1. *Z*-scores were calculated using a between-subjects fixed-effects GLM on all 12 subjects' individual correlation maps, in standard (MNI) space.

Table 2

Peak correlation coordinates: 6 cortical regions

Anatomical label		*x*	*y*	*z*	*Z*-score
Visual area MT correlations					
V/VI	L	−18	−72	−18	3.92
	R	16	−68	−16	3.81
VIII	L	−14	−74	−52	2.81
Superior temporal/auditory correlations					
V/VI	L	−20	−64	−16	2.80
	R	18	−60	−16	2.11
Somatosensory correlations					
V/VI	L	−20	−58	−18	3.40
	R	20	−64	−18	2.52
VIII	L	−22	−52	−60	2.49
	R	24	−62	−58	1.97
Motor/premotor correlations					
V/VI	L	−20	−52	−20	3.36
	R	34	−48	−26	2.48
VIII	L	−22	−54	−60	2.13
	R	30	−58	−62	2.64
Posterior-parietal correlations					
VIIa (paravermal)	L	−10	−88	−34	3.09
	R	14	−86	−42	2.60
Crus II	L	−44	−68	−52	3.64
	R	42	−70	−50	2.40
Prefrontal correlations					
VIIa (paravermal)	L	−8	−86	−44	3.24
	R	12	−88	−42	2.75
Crus I	L	−32	−64	−32	2.48
	R	28	−70	−30	3.32
Crus II	L	−42	−74	−48	3.74
	R	38	−72	−50	3.95

Note: This table gives MNI coordinates for the voxel with the peak *Z*-score in each cluster for the correlation maps corresponding to 6 cortical regions, that is, the results of Analysis 3. *Z*-scores were calculated using a between-subjects fixed-effects GLM on all 12 subjects' individual correlation maps, in standard (MNI) space.

Table 3

Peak correlation coordinates within the prefrontal and posterior-parietal cortex

Anatomical label		*x*	*y*	*z*	*Z*-score
Correlations in prefrontal cortex					
Posterior medial frontal gyrus (area 8)	L	−36	14	56	3.76
	R	38	16	54	4.02
Middle medial frontal gyrus (area 9/46)	L	−36	28	46	3.85
	R	24	28	48	3.29
Frontal pole	L	−26	56	24	4.17
	R	40	54	16	4.42
Correlations in posterior-parietal cortex					
Inferior parietal lobule	L	−48	−64	50	4.18
	R	48	−62	50	4.72
Medial superior parietal lobule (area 7b, M)	M	4	−72	44	4.74
Posterior cingulate	M	−2	−28	38	3.90

Note: This table shows the regions in the prefrontal and posterior-parietal cortex which were most strongly correlated with a subregion of the cerebellum: that is, the results of Analysis 4. The subregions of the cerebellum used comprised those voxels identified as having significant correlation with the prefrontal and parietal masks as a whole, in Analysis 3. MNI coordinates are given for the voxel with the peak *Z*-score in each cluster; *Z*-scores were calculated using a between-subjects fixed-effects GLM on all 12 subjects' individual correlation maps, in standard (MNI) space.

different broad functional zones of cerebral cortex. As in Analysis 1, they were created by combining masks from the Harvard–Oxford structural atlas. The masks were prefrontal cortex (as described in Analysis 1, above); motor/premotor cortex (as described in Analysis 1, above); somatosensory cortex (all the lateral cortex lying posterior to the fundus of the central sulcus and anterior to the fundus of the postcentral sulcus), posterior-parietal cortex (all the lateral cortex posterior to the postcentral sulcus and anterior to the parieto-occipital sulcus, and the corresponding tissue on the medial surface extending to the paracingulate sulcus on the medial surface); visual area MT/V5 (this mask was taken from the Jülich Histological atlas, using the voxels for which MT was the classification with the highest probability); superior temporal cortex including auditory cortex and adjacent association cortex (temporal lobe cortex superior to the superior temporal sulcus, including the planum temporale).

The data set and preprocessing were as in Analysis 1. The voxelwise correlation mapping procedure was as described in Analysis 1, but each cortical mask was processed in a separate analysis run, with the effect that at each cerebellar voxel the correlation with each cortical mask was calculated separately: the correlations with other cortical masks were *not* partialled out as in Analyses 1 and 2 (although the confound time series relating to white matter, CSF, and motion were partialled out as in Analysis 1). Thus, the correlation maps generated in this analysis could include voxels which have a high resting state correlation with more than one cortical mask. The reason for this approach was to visualize overlap between the RSNs of different cortical systems as well as the difference between them (e.g., somatosensory and motor regions of the cerebellum are known to overlap—see Discussion).

Analysis 4: Projecting Correlations Back on Prefrontal and Parietal Cortex

To do this we reversed the strategy of the previous analyses. We defined prefrontal and parietal zones in the cerebellar cortex, based on the results of Analysis 3, and extracted the first Eigen time series from these masks. The original prefrontal and posterior-parietal cerebral–cortical masks now took the role of voxels to be classified. This reverse approach allowed us to probe which voxels within the cerebral–cortical masks drove the correlation with the cerebellum.

The cerebellar masks were defined from the group *Z*-score maps from Analysis 3, corresponding to the prefrontal and posterior-parietal cerebral–cortical masks. Voxels with a *Z*-score above 1.6 (equivalent of $P < 0.05$ uncorrected) were included in the cerebellar masks—that is, all those voxels shown in the correlation map for prefrontal or parietal cortex in Figure 3 were included. The cerebellar masks were not binarized, so those voxels with a stronger *Z*-statistic for correlation with the cortical masks contributed more strongly to the calculation of the Eigen time series. The cerebellar "prefrontal zone" mask included a large part of Crus II, a smaller area in Crus I, and a third peak in paravermal Lobule HVIIa. The cerebellar "posterior-parietal zone" mask was similar, except that the contribution of Crus I was much weaker (see Fig. 3 and Table 2).

The data set was the same one used in Analysis 1. Preprocessing and analysis techniques were as in Analysis 1, but note the reversal of roles of cortical and cerebellar masks.

Note that this approach is roughly equivalent to correlating the original Eigen time series derived from the prefrontal and posterior-parietal ROIs with each voxel in the cortex, as in the Supplementary Information, and the results of the 2 analyses are correspondingly similar.

Results

Results 1. Motor and Prefrontal Zones in Cerebellar Cortex

The cerebellar correlation maps generated by this analysis are shown in Figure 1; peaks of correlation are given in Table 1. Voxels which had strong resting functional connectivity with the prefrontal cortex were found mostly in the posterior cerebellum and particularly in Lobule HVIIa, Crus II, with a smaller region in Crus I and a few significantly correlated voxels in Lobule HIX (i.e., the tonsil). For the motor mask, the strongest resting state functional connectivity was in Lobule HVI, extending into Lobule HV and (marginally) Lobule HIV. A second motor-correlated region was present in Lobule HVIII. In all cases the zones of correlation were largely symmetrical across the left- and right-cerebellar hemispheres.

Results 2: Lateralization of Cerebro-cerebellar Connectivity

The results of this analysis are shown in Figure 2. The lateralized correlation analysis indicated a contralateral mapping between cortical masks and strength of correlation in the cerebellum. That is, for the right-hemisphere cortical masks, correlation was stronger in the left cerebellum and vice versa.

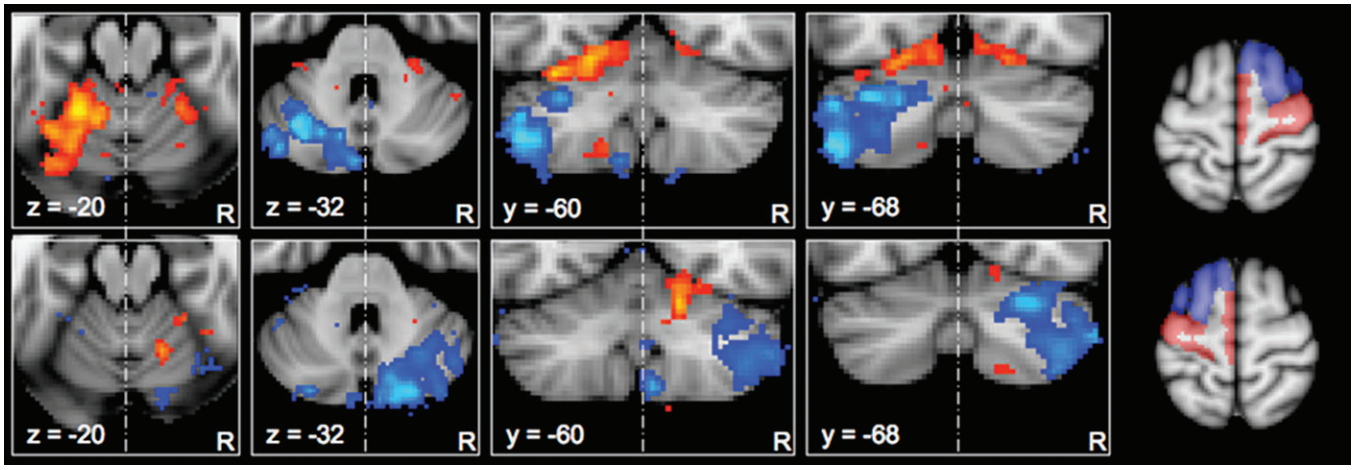

Figure 2. Lateralization of correlation maps for motor and prefrontal targets. Correlation maps for unilateral cortical masks in standard (MNI) space showing the voxel-wise significance (*Z*-score) of the correlation with prefrontal (blue) and motor/premotor (red) masks. Maps are thresholded at $Z > 1.6$ (equivalent of $P < 0.05$ uncorrected) and presented with the left hemisphere to the left of the image. Top row: Maps corresponding to the masks in the right cerebral hemisphere. Bottom row: Maps corresponding to the masks in the left cerebral hemisphere. The corresponding cortical masks are shown to the right of the figure. Note the relative strength of functional connectivity in the cerebellar hemisphere contralateral to the cortical mask. Maps represent *only* lateralized correlations, as correlations shared between cortical masks were partialled out (see Methods). Z-score scales are as in Figure 1.

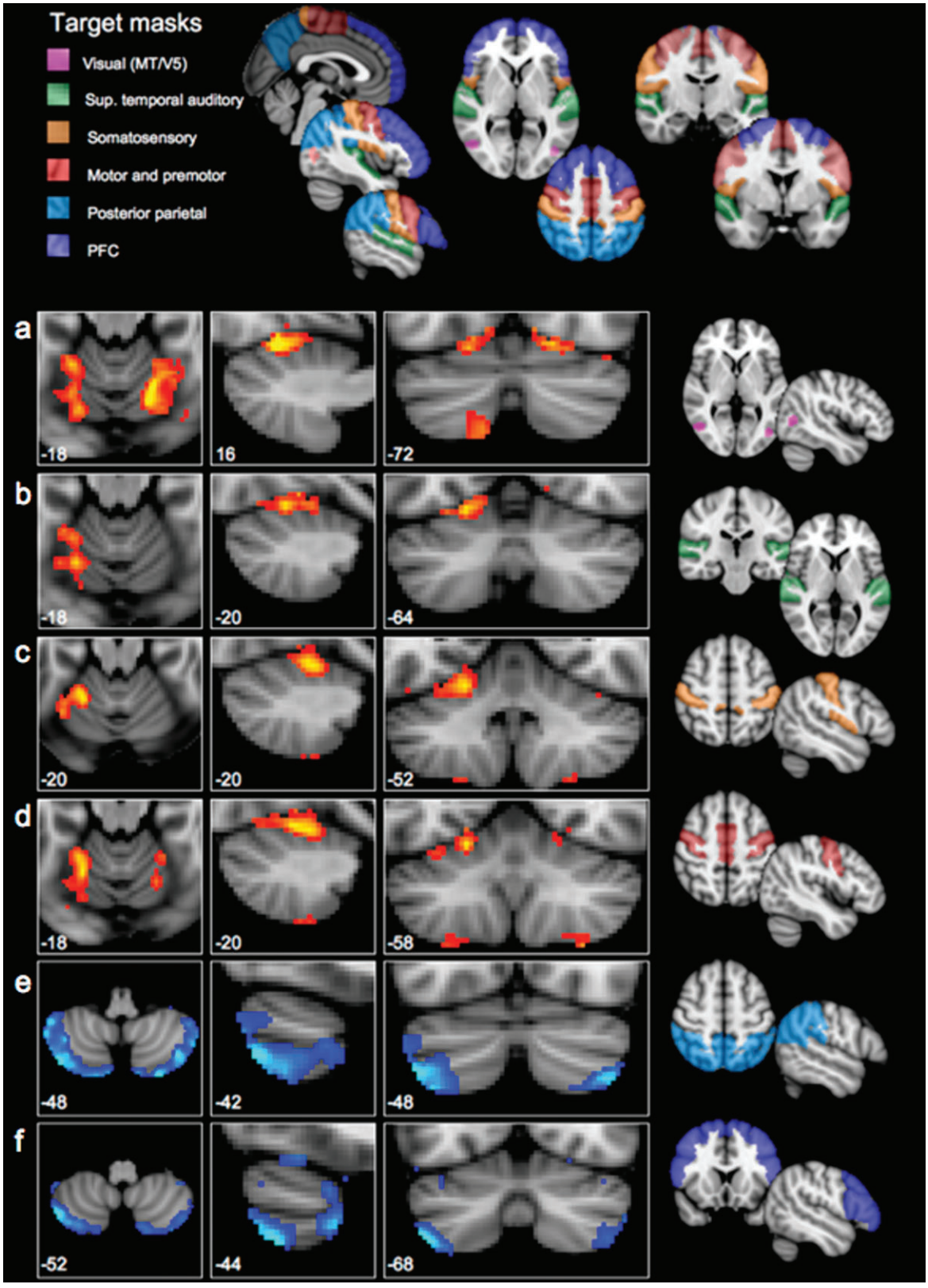

Figure 3. Correlation maps for 6 cortical regions. Presented in panels (*a*–*f*) are group correlation maps in standard (MNI) space, showing the voxel-wise significance (*Z*-score) of the correlation with each of 6 cortical masks in the cerebral cortex—from top to bottom, (*a*) visual area MT, (*b*) superior temporal cortex, (*c*) somatosensory cortex, (*d*) motor and premotor cortex, (*e*) posterior-parietal cortex, and (*f*) prefrontal cortex. Maps are thresholded at $Z > 1.6$ (equivalent of $P < 0.05$ uncorrected) and presented with the left cerebellar hemisphere to the left of the image. Each row corresponds to one cortical mask; the mask is shown to the right of the row. The set of cortical masks are shown together in the top panel. Note that the correlation maps fall into 2 patterns, shown in blue and red colorways above: the correlation maps for visual, auditory, somatosensory, and motor cortices were highly similar, and different from the correlation maps for prefrontal and posterior-parietal cortex, which in turn were similar to each other.

In each case, *within* the active cerebellar hemisphere, the pattern of activity was observed as in Analysis 1: that is, Lobules HV, HVI, and HVIII correlated with the motor cortex and Crus I and II correlated with the prefrontal mask.

Quantitative comparison of the strength of correlation between cerebellar ROIs and the 2 cortical hemispheres revealed a highly significant lateralization effect for the connectivity of Crus I/II in both cerebellar hemispheres (i.e., the correlation between each Crus I/II mask and the contralateral prefrontal mask was much greater than the correlation with the ipsilateral mask)—$P < 0.00001$ in both cases. For the superior cerebellar ROIs, the pattern was statistically weaker—contralateral correlations were significantly stronger than ipsilateral correlations for the left cerebellar region of interest ($P < 0.00001$), but, although contralateral correlations were greater than ipsilateral correlations for the right superior cerebellum (see Fig. 2), this lateralization was not statistically significant ($P = 0.245$).

Results 3: Six Cortical Masks

The correlation maps corresponding to the 6 cortical regions are shown in Figure 4; coordinates of peak correlations are given in Table 2. The correlation maps for visual area MT, auditory (superior temporal), somatosensory, and motor/premotor cortex were similar: in each case, Lobule HVI showed the strongest correlation with the cortical region. For the motor/premotor, visual, and somatosensory masks, correlations were also observed in Lobule HVIII. The correlation maps for prefrontal and posterior-parietal masks had peaks in Crus II, with further peaks in Crus I for the prefrontal cortex.

Results 4: Projecting Correlations Back onto Prefrontal and Parietal Cortex

The correlation maps across prefrontal and posterior-parietal cortex, which show the voxels correlating most strongly with the cerebellar prefrontal and posterior-parietal zones, are shown in Figure 4; coordinates of peak correlation are given in Table 3. In the prefrontal cortex, the region correlated with the cerebellum included the majority of the superior and middle frontal gyri and the frontal pole, with a posterior peak of correlation lying near the anterior border of area 8, a more anterior peak in area 9/46 (as described by Petrides and Pandya 1999) and a third peak in the frontal pole; the pattern of correlation was largely bilateral. The inferior frontal gyrus (Brodmann areas 44, 45, and 47) did not correlate significantly with the cerebellar prefrontal zone. In the lateral parietal cortex, the inferior, but not superior parietal lobule was correlated with the cerebellar parietal zone—the boundary of the significant correlation map corresponded closely to the intraparietal sulcus (see Fig. 4). However, the medial aspect of the superior parietal lobule (posterior part) was correlated with the cerebellum.

Discussion

The results of the 4 analyses, taken together, indicate that the cerebellar cortex can be divided into at least 2 functional zones based on their resting-state functional connectivity: a primary sensorimotor zone, having functional connectivity with motor and premotor cortex, somatosensory, visual, and auditory cortex; and what we might term a supramodal zone, having functional connectivity with dorsolateral prefrontal and inferior posterior-parietal regions which are not closely linked to sensory or motor processing. The primary sensorimotor zone incorporates the superior lobules of the cerebellar hemispheres (Lobules HV and HVI) and Lobule HVIII. The supramodal zone is restricted to Lobule HVIIa, with the strongest prefrontal and posterior-parietal connectivity in Crus II of Lobule HVIIa. Within each of these zones, there are overlapping connectivity maps for several cortical regions. Connectivity maps for visual, auditory, somatosensory, and motor

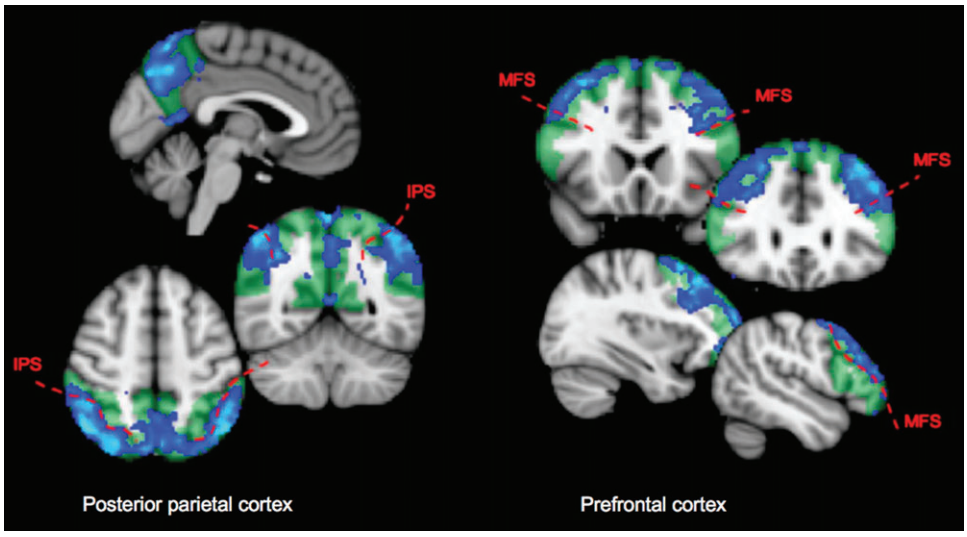

Figure 4. Prefrontal and posterior-parietal subregions contributing to resting state connectivity with the posterior cerebellum. These connectivity maps were generated by taking the first Eigen time series from the cerebellar supramodal zone, and identifying voxels in the prefrontal and posterior-parietal cortex which correlated with it. Hence, they indicate which voxels within the cerebral–cortical regions contribute to the resting state correlation with the posterior cerebellum. Green tinted regions show the extent of the cortical regions. Blue statistic maps indicate group *Z*-scores thresholded at $Z > 1.6$ (equivalent of $P < 0.05$ uncorrected). Note that even at this low threshold, the parietal correlation map is limited to the inferior parietal lobule and medial parietal cortex—there is a clear boundary between significant and nonsignificant correlation at the intraparietal sulcus (especially clear on axial view). The prefrontal correlation map does not extend into the inferior frontal gyrus; a boundary at the inferior frontal sulcus is clearly visible in the coronal views. MFS, medial frontal sulcus; IPS, intraparietal sulcus.

cortex overlap in the primary sensorimotor zone; connectivity maps for prefrontal and posterior-parietal cortex overlap in the supramodal zone.

Compatibility with Previous Models

The results described here are largely compatible with Schmahmann's schema in which the cerebellum can be divided into motor and executive zones (e.g., Schmahmann and Sherman 1998), and with the parallel circuits model of Strick and colleagues (e.g., Dum and Strick 2003), which also suggests that separate functional zones should be present within cerebellar cortex. However, there are some aspects of the present findings which should be discussed in relation to the models of Schmahmann (e.g., Schmahmann and Sherman 1998; Schmahmann and Caplan 2006) and Strick (e.g., Middleton and Strick 1997; Dum et al. 2002).

First, the precise location of primary and supramodal zones: Schmahmann describes a relationship between the anterior lobe of the cerebellum and motor function, and between the posterior lobe and executive function (see Introduction). The anterior lobe of the cerebellum is, strictly speaking, limited to the lobules anterior to the primary fissure (that is Lobles I–V), and the posterior lobe comprises Lobules VI–X. In contrast, we observed the anterior boundary between sensorimotor and supramodal zones to lie at the superior-posterior fissure, that is, between Lobule VI and Lobule VIIa/Crus I. We also observed a second primary sensorimotor zone within the posterior cerebellum, in Lobule HVIII. Thus, our supramodal zone was limited to Lobule HVIIa, Crus I and II, not the whole posterior cerebellum.

The pattern of functional connectivity observed in the present study is, however, compatible with longstanding observations that there are sensori-motor representations of the body in both the superior cerebellum (Lobules IV–VI) and inferior cerebellum (Lobules HVIIb and HVIII)—evoked potentials following peripheral tactile stimulation were first observed in the 1940s (Adrian 1943; Snider and Stowell 1944), and later it was confirmed that the representations could be activated by stimulating the cerebral-cortical motor and somatosensory areas (Allen et al. 1974; Allen et al. 1979; Snider and Eldred 1952). More recently, the same pattern has been confirmed in the human brain in functional imaging studies (e.g., Jueptner et al. 1997; Bushara et al. 2001; Grodd et al. 2001; Thickbroom et al. 2003), and white matter connections from motor cortex to Lobles HIV–HVI and HVIII have been traced in the monkey (Kelly and Strick 2003, Lu et al. 2007). The concentration of supramodal projections in Crus II was confirmed by the anatomical work of Kelly and Strick (in the case of prefrontal cortex), whereas in an electrophysiological study, stimulation of parietal association cortex in the cat excited cells in Crus I and II, whereas cells in Lobules IV–VI and HVIII were more readily excited by stimulation of motor cortex (Sasaki et al. 1975).

In relating the present work to patient studies, however, it is worth noting that in the human brain Crus I and II make up the large majority of the volume of the cerebellum posterior to Lobule VI. Thus, in terms of the tissue lost in lesions of the posterior cerebellum in human patients, motor representations in Lobule HVIII would be a relatively minor component.

Second, although our results support Strick's model of parallel circuits for prefrontal and motor cerebro-cerebellar connectivity, we also observed considerable *overlap* between the functional connectivity maps for some cortical regions: that is, sensory and motor cortical regions roughly shared one cerebellar map, whereas prefrontal and posterior-parietal cortex shared a second, separate cerebellar map. This overlap was observed when partial correlations between cortical masks were not removed from the data—indicating that some voxels had correlations with 2 sensory (or 2 supramodal) cortical masks. How can this overlap be reconciled with the parallel circuits model? First, note that the parallel circuits observed by Strick and colleagues pertained to motor and prefrontal connections, not to sensory connections (which were not traced). When Clower et al. (2005) investigated the dentate connectivity of a *parietal* region, aIP, they noted that instead of having a discrete output channel from the cerebellum, aIP also received connections from regions of the dentate projecting to other areas of cerebral cortex, including M1 and ventral premotor cortex. In other words, they observed a degree of overlap between cortico-cerebellar circuits when cerebellar outputs were going to *functionally related* cerebral areas.

The present results suggest that although there are parallel circuits for supramodal/executive and motor functions, information from sensory and motor areas of cerebral cortex is actually brought *together* in the sensorimotor zone of the cerebellum—at least, the same set of voxels share connections with several cortical systems (note that the resolution of fMRI is insufficient to determine how the inputs are integrated at a microcircuit level). This is in accordance with electrophysiological studies, in which evoked potentials were observed in Lobules V and VI following peripheral visual, auditory and somatosensory stimulation (Snider and Eldred 1952). In a popular model of cerebellar function, the cerebellum computes forward models of motor behavior (Wolpert and Miall 1996); sensory feedback is required to set up and refine such a model. Furthermore, output from an internal forward-model can be used to "cancel out" sensory feedback caused by one's own actions—for example, in self-tickling, increased activity in the superior cerebellum is associated with decreased activity in somatosensory cortex and decreased ticklish sensation (Blakemore et al. 1999). Indeed, it has been proposed that sensory processing, not motor control, is the main function of cerebellar sensorimotor circuits (Bower 1997). It seems, therefore, that the cerebellum brings together motor and sensory information to predict the effects of motor commands on both body position and sensory processing. (Strick and colleagues [e.g., Dum and Strick 2003] observed separate output channels in the dentate nucleus for different effectors [i.e., within the channel for M1, they observed separate channels for connections to hand, face, and leg areas]. It is tempting to suggest that connections with somatosensory cortex should overlap with these motor output channels, but keeping the same strict somatotopy. However, note that the present study only indicates correlations between cerebral and cerebellar-*cortical* activity, which must be mediated by multi-synaptic circuits. The method used here cannot indicate how sensory and motor information enters the cerebellum—e.g., some computational models of cerebellar microcircuits suggest that sensory information used to refine forward models [i.e., as an error signal] would be carried in climbing fibers, arising in the inferior olive [i.e., it would bypass the pons]. Therefore, the presence of overlapping resting-state networks does not

necessarily predict a certain organization of cells in the pons or dentate nucleus.) This cancellation, or error detection, may arise from the convergence of mossy fiber inputs from cerebral cortex, climbing fiber inputs via the inferior olive, and feedback from the peripheral nervous system—all of these inputs are thought to converge on a similar somatotopic map in the sensorimotor part of the cerebellum (Provini et al. 1968; Andersson and Nyquist 1983); the resting state connectivity observed in the present study could arise from the cortico-pontine or cortico-olivary pathway, or likely both.

Visual and Auditory Functional Connectivity

As well as somatosensory and motor/premotor cortex, the primary sensorimotor zone has resting functional connectivity with visual area MT and the superior temporal cortex, including auditory cortex and auditory association cortex. Connections from both areas have been traced to the pons (MT: Glickstein et al. 1994; superior temporal cortex: Schmahmann and Pandya 1991, 1992). This probably reflects the importance of visual and auditory information in motor control. For example, the cerebellum is essential to calibrate the relationship between visual and somatosensory/motor information—this can be seen in experiments with prismatic glasses (Pisella et al. 2005; Luauté et al. 2009). In terms of superior-temporal connectivity, the cerebellum may be involved in relating auditory feedback to motor control in speech (Watkins et al. 2008). Interestingly, although present, the connections from superior temporal cortex to the pons were relatively weak in the monkey (Schmahmann and Pandya 1991). We might hypothesize that cerebellar-auditory connections would be stronger in the human, reflecting the role of the cerebellum in speech production.

The Supramodal Zone of the Cerebellum

Using resting state functional connectivity, we identified a "supramodal zone" in the posterior cerebellum, largely in Crus II. This region of the cerebellum had strong functional connectivity with the prefrontal and posterior-parietal cerebral–cortical regions.

It has been argued (Glickstein 2007) that frontal and parietal connections with the cerebellum are dominated by subregions involved in motor control, such as the frontal eye fields. However, when we mapped the strength of resting state correlation with the posterior cerebellum across our prefrontal and parietal masks (Analysis 4), the regions with the strongest cerebellar correlation were those which are *not* closely involved in sensory or motor processing. In the prefrontal cortex, the entire middle and superior frontal gyri, and the frontal pole, showed strong correlation with the posterior cerebellar supramodal zone. In contrast, no significant correlation was observed in the region at the posterior border of prefrontal cortex (area 8/6 border), described by Paus (1996) to contain the human frontal eye fields, although a peak was observed toward the anterior border of area 8. Neither did the inferior frontal gyrus, containing Broca's area (which is implicated in fine motor control) show significant correlation with the posterior cerebellum—this is in accordance with tracer work in monkeys (Glickstein et al. 1985; Schmahmann and Pandya 1997) and degeneration studies in humans (Beck 1950), in which pontine projections were found to be much stronger from the dorsolateral than ventrolateral prefrontal cortex in the monkey (although Schmahmann and Pandya did observe weak connections from Broca's area to the pons, so the present results may reflect the dominant rather than exclusive connectivity pattern).

In the parietal cortex, the significant correlation with the posterior cerebellum was limited to the inferior parietal lobule (Fig. 4). The inferior parietal cortex has been implicated in executive functions such as attentional orienting (Corbetta et al. 2000; Kincade et al. 2005) and theory of mind (Saxe and Kanwisher 2003; Young and Saxe 2009). In contrast, the superior parietal cortex (which was not significantly correlated with the posterior cerebellum in the present analysis) is thought to contain regions homologous to the monkey IPS areas involved in the planning of movement such as LIP, MIP, and VIP (see Culham and Valyear 2006 for review).

Are these supramodal connections supported by prior anatomical evidence? Tracer studies indicate that connections between the dorsolateral prefrontal cortex and cerebellum do exist in monkeys: Glickstein et al. (1985) first observed prefrontal-pontine projections, and Schmahmann and Pandya (1997) confirmed that cells in the pontine nuclei were labeled even after injections of tracer into anterior parts of dorsolateral prefrontal cortex which were distant from the frontal eye fields. Several studies from Strick's group have indicated connections from the ventral dentate (Dum et al. 2002; Middleton and Strick 2001) or Crus II of cerebellar cortex (Kelly and Strick 2003) to dorsolateral prefrontal cortex. Meanwhile, electrical stimulation of parietal association cortex elicits evoked potentials in the cat cerebellum, Crus I and II (Sasaki et al. 1975).

In the monkey, the prefrontal cortex makes up a relatively minor proportion of cerebellar input compared with motor and premotor cortex. However, supramodal cortico-cerebellar connections may be more substantial in the human brain than the monkey: The region of cerebellar cortex which connects with prefrontal cortex is enlarged in monkeys compared with cats, and is much larger in humans than in monkeys (Ramnani 2006). In parallel, the proportion of white matter in the cerebral peduncle (a major tract from the cerebral cortex to the cerebellum) arising from the prefrontal cortex is larger in humans than in macaque monkeys (Ramnani et al. 2006). Therefore, although the proportion of the cerebellum falling in the supramodal zone in the present study is strikingly large (see Fig. 2), in fact the difference from known monkey anatomy is quantitative—the same lobules are involved in both species (Lobule HVIIa, mainly Crus II).

Our findings indicate that the posterior cerebellar supramodal zone is genuinely associated with "higher order" association cortex. Nonetheless, note that in the analysis of which parietal and prefrontal areas drive the connectivity with posterior cerebellum (Analysis 4), we explicitly looked for those voxels correlating with an Eigen time series derived from the posterior cerebellum (Crus II). The mask from which that time series was obtained was defined as the voxels having a significant correlation with the first Eigen time course of the prefrontal- or posterior-parietal cortical mask. Therefore, although our results confirm that a region of the cerebellum exists which has strong resting functional connectivity with nonmotor regions of prefrontal and parietal cortex, it does not rule out the possibility that regions of the parietal and prefrontal cortex which are more closely involved in sensorimotor function *also* participate in a separate RSN with a different cerebellar subregion.

Regions Not Correlated with Any Mask

Some parts of the cerebellum did not show significant correlation with any mask in our analyses—notably, Lobules I–III and most of Lobule IV, parts of Lobule VIII, medial Lobule IX (the uvula) and the entire vermis. The masks used here do not cover the entire brain, but rather represent some functionally distinct systems which are known to have significant connections with the cerebellum. It is therefore possible that the unlabeled parts of the cerebellum receive input from parts of the cerebral cortex which were not included in the masks. Alternatively, these areas may have connections limited to subcortical nuclei, or inputs dominated by peripheral receptors (the body and sense organs). It is also possible that some cortical time series, which would have contributed to cortico-cerebellar functional connectivity, were "swamped" by the inclusion of more than one functional region in a cortical mask. In future, approaches may be developed in which the cortical subdivisions and cerebellar subdivisions are both defined in a data-driven way; such a data-driven approach would allow a more comprehensive parcellation of the cerebellum.

Caveats and Benefits of the Resting State Functional Connectivity Method

Resting-state functional connectivity is not a direct measure of anatomical connectivity. Although anatomical connectivity (assessed with diffusion weighted imaging tractography) is strongly correlated with resting state functional connectivity (Hagmann et al. 2008), both diffusion tractography and resting-state connectivity can reflect multisynaptic connections. Thus, there are 3 important caveats in the interpretation of resting state "connectivity." First, we do not know the *direction* of information flow between cerebral and cerebellar cortices (the parallel circuits model suggests that cerebro-cerebellar connections are likely to be bidirectional so the flow of information could be either way). Second, some of the cerebral–cortical areas having strong resting state functional connectivity with the cerebellum may only share information with the cerebellum via a mediating cortical or subcortical area (although all areas described in this paper are known to have anatomical connections with the pons or dentate). Third, resting-state correlations cannot indicate the route which multisynaptic connections take from the cortex to the cerebellum or vice versa. The anatomical connections linking cerebral- and cerebellar cortex in a RSN could be afferents via the pons or the inferior olive, or efferents via the dentate, or indeed all 3 (as we might expect from the parallel circuits model).

Despite these limitations, it is a strength of the resting state approach that RSNs give an immediate measure of *functional* cohesion—even if this is mediated by multisynaptic pathways—and thus anatomical and functional measures might be regarded as complimentary. For example, say a cortical area X has anatomical connections with 4 other cortical regions A, B, C, and D. Should these 5 regions be viewed as a single network, or is it possible that the central "node" participates in 2 functionally distinct networks, AXB and CXD? Resting state analysis can distinguish between these 2 hypotheses because it takes account of the changing pattern of relationships between areas over time.

In the specific case of the cerebellum, the resting-state approach is particularly valuable for 2 reasons. First, because of the difficulty in mapping connections of the cerebellar cortex with traditional anatomical methods (discussed above). Second, using fMRI allows us to study the functional organization of the cerebellum in the *human* brain. This is interesting because there are morphological differences between the human cerebellum and those of other species—quantitatively, the supramodal zone (Crus I and II) of the cerebellum is much bigger in humans than macaques—the difference is comparable to the difference in size between the human and monkey prefrontal cortices (Ramnani 2006). There are also topographical differences in the organization of cortico-pontine projections between cats and monkeys (Brodal 1978). In primates, the cerebellum is important in fine motor control and tactile exploration with the fingertips (Gao et al. 1996). In humans, it is possible the cerebellum also plays a role in the production of speech (another behavior requiring fine motor control). Thus, although it seems likely that the computational function of cerebellar microcircuits is conserved across species, the relative importance of different cortical inputs might be expected to differ between species in line with differences in behavior and sensory acuity.

Using the resting-state approach, we were able to replicate the pattern of connectivity between cerebellar- and cerebral cortex observed by Kelly and Strick (2003), and found the expected pattern of lateralization of connections. Having validated the method against existing data, we went on to expand our analysis to more cortical regions, and to identify which parts of our cortical masks drove cerebellar connectivity. Overall, the results provide further support for the growing body of anatomical, clinical, and neuroimaging findings which suggest regional differences within the cerebellum.

Conclusions

The human cerebellum can be divided into at least 2 zones based on resting-state functional connectivity: 1) A primary sensorimotor zone, having strong functional connectivity with motor and premotor cortex, somatosensory cortex, and some visual and auditory regions. 2) A supramodal zone, having strong resting state functional connectivity with the prefrontal and parietal cortex. Each of these zones contains overlapping connectivity maps for different cortical areas—primary sensory and motor zones, and supramodal association cortex, respectively.

Supplementary Material

Supplementary material can be found at: http://www.cercor.oxfordjournals.org/.

Funding

Biotechnology and Biological Sciences Research Council grant (BBS/B/16313 to H.J.B.); Wellcome Trust grant (070204/z/05/z to H.J.B.); NIHR Biomedical research centre funding (to C.B.); MS Society Italy and UK grant (to V.T. and H.J.B.).

Notes

Thank you also to Paul Matthews. *Conflict of Interest*: None declared.

Address correspondence to Jill O'Reilly, BA, MSc, DPhil, FMRIB Centre, John Radcliffe Hospital, Headley Way, Headington, Oxford OX3 9DU, UK. Email: joreilly@fmrib.ox.ac.uk.

References

Adrian ED. 1943. Afferent areas in the cerebellum connected with the limbs. Brain. 66:289–315.

Allen GI, Azzena GB, Ohno T. 1974. Cerebellar Purkyně cell responses to inputs from sensorimotor cortex. Exp Brain Res. 20(3):239–254.

Allen GI, Azzena GB, Ohno T. 1979. Pontine and non-pontine pathways mediating early mossy fiber responses from sensorimotor cortex to cerebellum in the cat. Exp Brain Res. 36(2):359–374.

Andersson G, Nyquist J. 1983. Origin and sagittal termination areas of cerebro-cerebellar clibing fibre paths in the cat. J Physiol. 337:257–285.

Andersson JLR, Jenkinson M, Smith SM. 2007. Non-linear registration, aka Spatial normalisation. FMRIB technical report TR07JA2, 2007.

Beck E. 1950. The origin, course and termination of the prefronto-pontine tract in the human brain. Brain. 73(3):368–391.

Beckmann CF, DeLuca M, Devlin JT, Smith SM. 2005. Investigations into resting-state connectivity using independent component analysis. Philos Trans R Soc Lond B Biol Sci. 360(1457):1001–1013.

Biswal B, Yetkin FZ, Haughton VM, Hyde JS. 1995. Functional connectivity in the motor cortex of resting human brain using echo-planar MRI. Magn Reson Med. 34(4):537–541.

Blakemore SJ, Wolpert DM, Frith CD. 1999. The cerebellum contributes to somatosensory cortical activity during self-produced tactile stimulation. Neuroimage. 10(4):448–459.

Bloedel JR. 1992. Functional heterogeneity with structural homogeneity: how does the cerebellum operate? Behav Brain Sci. 15:666–678.

Bower JM. 1997. Is the cerebellum sensory for motor's sake, or motor for sensory's sake: the view from the whiskers of a rat? Prog Brain Res. 114:463–496.

Brodal P. 1978. The corticopontine projection in the rhesus monkey: origin and principles of organization. Brain. 101:251–283.

Bushara KO, Wheat JM, Khan A, Mock BJ, Turski PA, Sorenson J, Brooks BR. 2001. Multiple tactile maps in the human cerebellum. Neuroreport. 12(11):2483–2486.

Clower DM, Dum RP, Strick PL. 2005. Basal ganglia and cerebellar inputs to 'AIP'. Cereb Cortex. 15(7):913–920.

Corbetta M, Kincade JM, Ollinger JM, McAvoy MP, Shulman GL. 2000. Voluntary orienting is dissociated from target detection in human posterior parietal cortex. Nat Neurosci. 3(3):292–297.

Damoiseaux JS, Rombouts SA, Barkhof F, Scheltens P, Stam CJ, Smith SM, Beckmann CF. 2006. Consistent resting-state networks across healthy subjects. Proc Natl Acad Sci USA. 103(37):13848–13853 Epub 2006 Aug 31.

Culham JC, Valyear KF. 2006. Human parietal cortex in action. Curr Opin Neurobiol. 16(2):205–212.

Desmond JE, Gabrieli JD, Wagner AD, Ginier BL, Glover GH. 1997. Lobular patterns of cerebellar activation in verbal working-memory and finger-tapping tasks as revealed by functional MRI. J Neurosci. 17(24):9675–9685.

Desmond JE, Gabrieli JD, Glover GH. 1998. Dissociation of frontal and cerebellar activity in a cognitive task: evidence for a distinction between selection and search. Neuroimage. 7(4 Pt 1):368–376.

Dum RP, Li C, Strick PL. 2002. Motor and nonmotor domains in the monkey dentate. Ann N Y Acad Sci. 978:289–301.

Dum RP, Strick PL. 2003. An unfolded map of the cerebellar dentate nucleus and its projections to the cerebral cortex. J Neurophysiol. 89(1):634–639.

Eccles JC, Ito M, Szentagothai J. 1967. The cerebellum as a neuronal machine. Berlin: Springer-Verlag.

Eickhoff SB, Stephan KE, Mohlberg H, Grefkes C, Fink GR, Amunts K, Zilles K. 2005. A new SPM toolbox for combining probabilistic cytoarchitectonic maps and functional imaging data. Neuroimage. 25(4):1325–1335.

Fox MD, Raichle ME. 2007. Spontaneous fluctuations in brain activity observed with functional magnetic resonance imaging. Nat Rev Neurosci. 8(9):700–711.

Friston KJ, Poline J, Holmes AP, Frith CD, Frackowiak. 1996. A multivariate analysis of PET activation studies. Hum Brain Mapp. 4(2):140–151.

Gao JH, Parsons LM, Bower JM, Xiong J, Li J, Fox PT. 1996. Cerebellum implicated in sensory acquisition and discrimination rather than motor control. Science. 272(5261):545–547.

Glickstein M. 2007. What does the cerebellum really do? Curr Biol. 17(19):R824–R827.

Glickstein M, May JG, 3rd, Mercier BE. 1985. Corticopontine projection in the macaque: the distribution of labelled cortical cells after large injections of horseradish peroxidase in the pontine nuclei. J Comp Neurol. 235(3):343–359.

Glickstein M, Gerrits N, Kralj-Hans I, Mercier B, Stein J, Voogd J. 1994. Visual pontocerebellar projections in the macaque. J Comp Neurol. 349(1):51–72.

Grodd W, Hulsmann E, Lotze M, Wildgruber D, Erb M. 2001. Sensorimotor mapping of the human cerebellum: fMRI evidence of somatotopic organization. Hum Brain Mapp. 13:55–73.

Hagmann P, Cammoun L, Gigandet X, Meuli R, Honey CJ, Wedeen VJ, Sporns O. 2008. Mapping the structural core of human cerebral cortex. PLoS Biol. 6(7):e159.

Ito M. 2008. Control of mental activities by internal models in the cerebellum. Nat Rev Neurosci. 9(4):304–313.

Jenkinson M, Smith SM. 2001. A global optimisation method for robust affine registration of brain images. Med Image Anal. 5(2):143–156.

Jueptner M, Ottinger S, Fellows SJ, Adamschewski J, Flerich L, Müller SP, Diener HC, Thilmann AF, Weiller C. 1997. The relevance of sensory input for the cerebellar control of movements. Neuroimage. 5(1):41–48.

Kelly RM, Strick PL. 2000. Rabies as a transneuronal tracer of circuits in the central nervous system (review). J Neurosci Methods. 103(1):63–71.

Kelly RM, Strick PL. 2003. Cerebellar loops with motor cortex and prefrontal cortex of a nonhuman primate. J Neurosci. 23(23):8432–8444.

Kincade JM, Abrams RA, Astafiev SV, Shulman GL, Corbetta M. 2005. An event-related functional magnetic resonance imaging study of voluntary and stimulus-driven orienting of attention. J Neurosci. 25(18):4593–4604.

Larsell O, Jansen J. 1972. The comparative anatomy and histology of the cerebellum. The human cerebellum, cerebellar connections and cerebellar cortex. Minneapolis (MN): The University of Minnesota Press.

Lu X, Miyachi S, Ito Y, Namby A, Takada M. 2007. Topographic distribution of output neurons in cerebellar nuclei and cortex to somatotopic map of primary motor cortex. Eur J Neurosci. 25:2374–2383.

Luauté J, Schwartz S, Rossetti Y, Spiridon M, Rode G, Boisson D, Vuilleumier P. 2009. Dynamic changes in brain activity during prism adaptation. J Neurosci. 29(1):169–178.

MacKay WA, Murphy JT. 1973. Activation of anterior interpositus neurons by forelimb muscle stretch. Brain Res. 56:335–339.

Middleton FA, Strick PL. 1997. Cerebellar output channels. Int Rev Neurobiol. 41:61–82.

Middleton FA, Strick PL. 2001. Cerebellar projections to the prefrontal cortex of the primate. J Neurosci. 21(2):700–712.

Noppeney U, Price CJ. 2002. A PET study of stimulus- and task-induced semantic processing. Neuroimage. 15(4):927–935.

Ojakangas CL, Ebner TJ. 1994. Purkinje cell complex spike activity during voluntary motor learning: relationship to kinematics. J Neurophysiol. 72(6):2617–2630.

Paus T. 1996. Location and function of the human frontal eye-field: a selective review. Neuropsychologia. 34(6):475–483.

Petrides M, Pandya DN. 1999. Dorsolateral prefrontal cortex: comparative cytoarchitectonic analysis in the human and the macaque brain and corticocortical connection patterns. Eur J Neurosci. 11(3):1011–1036.

Pisella L, Rossetti Y, Michel C, Rode G, Boisson D, Pélisson D, Tilikete C. 2005. Ipsidirectional impairment of prism adaptation after unilateral lesion of anterior cerebellum. Neurology. 65(1):150–152.

Provini L, Redman S, Strata P. 1968. Mossy and climbing fibre organization on the anterior lobe of the cerebellum activated by forelimb and hindlimb areas of sensorimotor cortex. Exp Brain Res. 6:216–233.

Ramnani N. 2006. The primate cortico-cerebellar system: anatomy and function. Nat Rev Neurosci. 7(7):511–522.
Ramnani N, Behrens TE, Johansen-Berg H, Richter MC, Pinsk MA, Andersson JL, Rudebeck P, Ciccarelli O, Richter W, Thompson AJ, et al. 2006. The evolution of prefrontal inputs to the cortico-pontine system: diffusion imaging evidence from Macaque monkeys and humans. Cereb Cortex. 16(6):811–818.
Ravizza SM, McCormick CA, Schlerf JE, Justus T, Ivry RB, Fiez JA. 2006. Cerebellar damage produces selective deficits in verbal working memory. Brain. 126:306–320.
Roskies AL, Fiez JA, Balota DA, Raichle ME, Petersen SE. 2001. Task-dependent modulation of regions in the left inferior frontal cortex during semantic processing. J Cogn Neurosci. 13(6): 829–843.
Sasaki K, Oka H, Matsuda Y, Shimano T, Mizuno N. 1975. Electrophysiological studies of the projections from the parietal association areas to the cerebellar cortex. Exp. Brain Res. 23:91–102.
Saxe R, Kanwisher N. 2003. People thinking about thinking people. The role of the temporo-parietal junction in "theory of mind". Neuroimage. 19(4):1835–1842.
Schmahmann JD. 1996. From movement to thought: anatomic Substrates of the cerebellar contribution to cognitive processing. Hum Brain Mapp. 4:174–198.
Schmahmann JD. 2004. Disorders of the cerebellum: ataxia, dysmetria of thought, and the cerebellar cognitive affective syndrome. J Neuropsychiatry Clin Neurosci. 16(3):367–378.
Schmahmann JD, Caplan D. 2006. Cognition, emotion and the cerebellum. Brain. 129(Pt 2):290–292.
Schmahmann JD, Doyon J, Toga AW, Petrides M, Evans A. 2000. MRI atlas of the human cerebellum. San Diego (CA): Academic Press.
Schmahmann JD, Pandya DN. 1992. Course of the fiber pathways to pons from parasensory association areas in the rhesus monkey. J Comp Neurol. 326(2):159–179.
Schmahmann JD, Pandya DN. 1991. Projections to the basis pontis from the superior temporal sulcus and superior temporal region in the rhesus monkey. J Comp Neurol. 308(2):224–248.
Schmahmann JD, Pandya DN. 1992. Course of the fiber pathways to pons from parasensory association areas in the rhesus monkey. J Comp Neurol. 326(2):159–179.
Schmahmann JD, Pandya DN. 1993. Prelunate, occipitotemporal, and parahippocampal projections to the basis pontis in rhesus monkey. J Comp Neurol. 337(1):94–112.
Schmahmann JD, Pandya DN. 1997. Anatomic organization of the basilar pontine projections from prefrontal cortices in rhesus monkey. J Neurosci. 17(1):438–458.
Schmahmann JD, Sherman JC. 1998. The cerebellar cognitive affective syndrome. Brain. 121(Pt 4):561–579.
Smith SM, Jenkinson M, Woolrich MW, Beckmann CF, Behrens TE, Johansen-Berg H, Bannister PR, De Luca M, Drobnjak I, Flitney DE, et al. 2004. Advances in functional and structural MR image analysis and implementation as FSL.. Neuroimage. 23(Suppl. 1):S208–S219.
Snider RS, Eldred E. 1952. Cerebro-cerebellar relationships in the monkey. J Neurophysiol. 15:27–40.
Snider RS, Stowell A. 1944. Receiving areas of the tactile, auditory and visual systems in the cerebellum. J Neurophysiol. 7:331–357.
Stoodley CJ, Schmahmann JD. 2009. Functional topography in the human cerebellum: a meta-analysis of neuroimaging studies. Neuroimage. 44(2):489–501Epub 2008 Sep 16.
Thickbroom GW, Byrnes ML, Mastaglia FL. 2003. Dual representation of the hand in the cerebellum: activation with voluntary and passive finger movement. Neuroimage. 18(3):670–674.
Watkins KE, Smith SM, Davis S, Howell P. 2008. Structural and functional abnormalities of the motor system in developmental stuttering. Brain. 131(1):50–59Epub 2007 Oct 10.
Wolpert DM, Miall RC. 1996. Forward models for physiological motor control. Neural Netw. 9(8):1265–1279.
Young L, Saxe R. 2009. An fMRI investigations of spontaneous mental state inference for moral judgement. J Cogn Neurosci. 21(7): 1396–1340.
Xiang H, Lin C, Ma X, Zhang Z, Bower JM, Weng X, Gao JH. 2003. Involvement of the cerebellum in semantic discrimination: an fMRI study. Hum Brain Mapp. 18(3):208–214.
Zhang Y, Brady M, Smith S. 2001. Segmentation of brain MR images through a hidden Markov random field model and the expectation maximization algorithm. IEEE Trans Med Imaging. 20(1):45–57.
Zhang D, Snyder AZ, Fox MD, Sansbury MW, Shimony JS, Raichle ME. 2008. Intrinsic functional relations between human cerebral cortex and thalamus. J Neurophysiol. 100:1740–1748.